Supplementary Information:

Expanding channels enhanced diffractive SAW actuated particle enrichment in vacuum-sealed microfluidic channels

David J. Bryan^{1,2}, Kirill Kolesnik³, Crispin Szydzik^{4,5}, Arnan Mitchell^{4,5}, Kelly L. Rogers^{1,2}, David J. Collins^{3,6*}

E-mail: david.collins@unimelb.edu.au

The perturbation approach

The piezoelectric actuator is driven by a time-harmonic AC-voltage with an oscillation frequency f and angular frequency $\omega = 2\pi f$. According to the perturbation approach, physical fields can be decomposed to initial, first and second-order terms $\overline{g} = \overline{g}_0 + \overline{g}_1 + \overline{g}_2$, where the 0-order term is the initial (background) condition. The first-order fields are time-dependent harmonic oscillations $\overline{g}_1(r,t) = g_1(r)e^{i\omega t}$ where $g_1(r)$ is the complex-valued amplitude. In the analysis, the first-order (linear) equations are solved to generate potential fields. By utilizing the phase-dependent factor $e^{i\omega t}$, the time-dependent solution can be produced. Throughout the study, the real-valued amplitude $g(r) = \text{Re}(g_1(r))$ will be discussed, as it corresponds to the amplitude in physical terms.

Governing equations

The acoustic field in the water domain is governed by the Navier-Stokes equation, the continuity equation, and the energy conservation equation:

$$\rho_0 \frac{\partial \mathbf{v}}{\partial t} = -\nabla p + \left(\mu' + \frac{\mu}{3}\right) \nabla(\nabla \cdot \mathbf{v}) + \mu \nabla^2 \mathbf{v},\tag{S1}$$

$$\frac{\partial \rho}{\partial t} = -\rho_0 \nabla \cdot \boldsymbol{v},\tag{S2}$$

$$\frac{\partial \rho}{\partial t} = -\rho_0 \nabla \cdot \boldsymbol{v}, \tag{S2}$$

$$\rho_0 C_p \frac{\partial T}{\partial t} - \alpha_p T_0 \frac{\partial p}{\partial t} = \nabla (D_T \nabla T), \tag{S3}$$

where ρ_0 is the mass density, ρ , v, T, p are the 1st-order harmonic perturbation of density, velocity, temperature and pressure respectively, bulk μ' and dynamic μ viscosities, C_p is the specific heat capacity at constant pressure, α_p is the thermal expansion coefficient, $T_0 = 293.15$ K is the ambient temperature, D_T is the thermal diffusivity of the liquid. The velocity perturbations v are related to those of pressure pthrough:

¹Walter and Eliza Hall institute of Medical Research, Parkville, Victoria, Australia

²Department of Medical Biology, University of Melbourne, Parkville, VIC, Australia

³Department of Biomedical Engineering, The University of Melbourne, Parkville, Victoria, Australia

⁴Integrated Photonics Applications Centre, RMIT, Melbourne, Victoria, Australia

⁵School of Engineering, RMIT University, Melbourne, VIC 3001, Australia

⁶Graeme Clarke Institute, University of Melbourne, Parkville, Victoria, Australia

^{*} Corresponding author

$$\mathbf{v} = i \nabla p \rho_0 \omega. \tag{S4}$$

Boundary conditions

The fluidic channel is enclosed with polydimethylsiloxane (PDMS) on the top and the sides, being common in SAW microfluidic devices. An impedance boundary condition for the first-order pressure p was accordingly set on these boundaries for the study:

$$\mathbf{n}\nabla p = i\frac{\omega\rho_0}{z_p}p,\tag{S5}$$

where n is the outward-pointing normal, $z_P = \rho_P c_P$ is acoustic impedance of PDMS, into which the acoustic wave is radiating. The SAW actuation on the Lithium Niobate, LiNbO₃, substrate was simulated with a velocity boundary condition on the bottom surface along y axis:

$$u_{\nu} = d_{\nu}\omega,$$
 (S6)

where d_{ν} is the boundary displacement amplitude.

The list of quantities and their values used in our simulations is given in Table S1. The first-order fields are solved for using the thermoviscous acoustics frequency domain using the built-in interface in COMSOL Multiphysics (Thermoacoustic module).

Acoustic radiation force

Particles suspended in the fluidic channel are subject to a time-averaged acoustophoretic radiation force F^{rad} . For a spherical particle with a diameter d_{ps} , this is given by Gor'kov, with

$$F^{rad} = -\nabla U^{rad}, \qquad U^{rad} = V_{ps} \left(\frac{1}{2} f_1 k_l \langle p^2 \rangle - \frac{3}{4} f_2 \rho_0 \langle \boldsymbol{v}^2 \rangle \right)$$

$$V_{ps} = \frac{\pi}{6} d_{ps}^3, \qquad f_1 = 1 - \frac{k_{ps}}{k_l}, \qquad f_2 = \frac{2(\rho_{ps} - \rho_0)}{2\rho_{ps} + \rho_0}, \qquad k_l = \frac{1}{\rho_0 c_l^2}, \tag{S7}$$

where U_{rad} is the Gor'kov potential, V_{ps} is a bead volume, f_1 and f_2 are monopole and dipole coefficients, k is compressibility, ρ is density, and the superscripts l and ps denote liquid and polystyrene beads respectively. The bracketed quantities denote the time average over one oscillation period of the complex time-harmonic, where for fields A and B, $\langle AB \rangle = 0.5Re(A^*B)$, where the asterisk denotes complex conjugation. Thus, the acoustophoretic force is calculated based on the computed first-order fields.

Acoustic contrast factor

An acoustic contrast factor can be used to describe the translation direction of particle motion in an acoustic potential field gradient. For the case of a sinusoidally varying pressure field, this can be expressed as

$$\phi = \frac{1}{3}f_1 - \frac{1}{2}f_2$$
, Eqn. S1

where substituting the relevant f_1 and f_2 expressions from Eqn. S7 yields the form of the expression in terms of the densities and compressibilities of the particle and fluid medium, more commonly seen in the acoustofluidic literature.

$$\phi = \frac{5\rho_p - 2\rho_m}{2\rho_p + \rho_m} - \frac{\beta_p}{\beta_m}$$

$$\beta = \frac{1}{\rho \cdot c_s^2}$$
(S8)

 Table S1. Material properties used in the computational study.

Parameter	Notation	Value
Frequency	f	19.66 MHz
Speed of sound of Lithium Niobate	c_{LN}	3931 m s ⁻¹
Density of Lithium Niobate	$ ho_{LN}$	4700 kg m ⁻³
SAW wavelength	λ_{SAW}	200 μm
Displacement amplitude	$d_{\mathcal{y}}$	0.05 nm
Speed of sound of liquid	c_l	1497 m s ⁻¹
Density of liquid	$ ho_0$	997 kg m ⁻³
Dynamic viscosity of liquid	μ	0.00089 Pa s
Bulk viscosity of liquid	μ'	0.00247 Pa s
Thermal conductivity of liquid	D_T	$0.603~{ m W}~{ m m}^{-1}{ m K}^{-1}$
Specific heat capacity of liquid	C_p	$4183 \text{ J kg}^{-1} \text{ K}^{-1}$
Thermal expansion coefficient of liquid	$lpha_p$	$0.000297~{ m K}^{\text{-1}}$
Speed of sound of PDMS	c_P	1054 m s^{-1}
Density of PDMS (10:1)	$ ho_P$	965 kg m ⁻³
Density of polystyrene beads	$ ho_{ps}$	1050 kg m^{-3}
Compressibility of polystyrene beads	k_{ps}	249 TPa ⁻¹

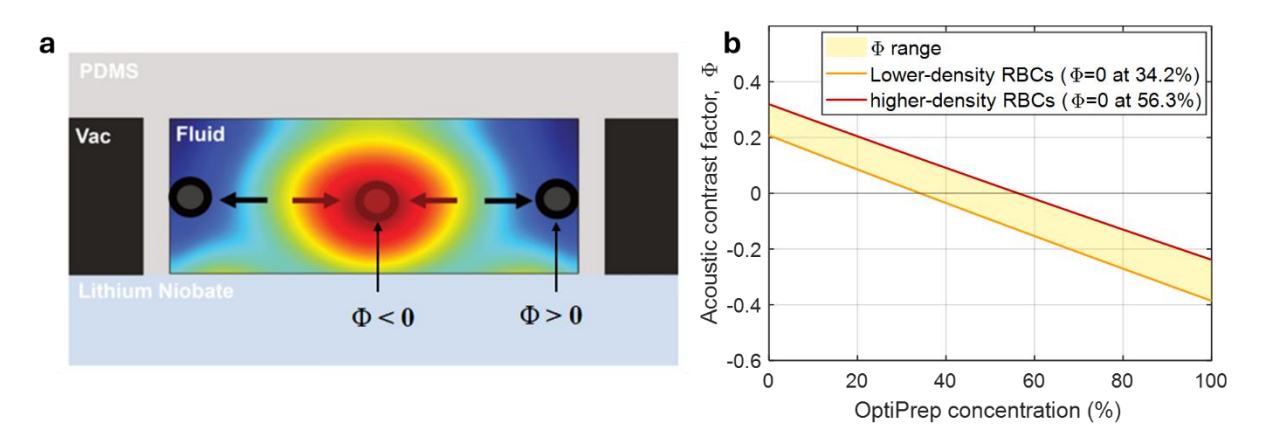


Figure S1: Modification of fluid media's acoustic properties. (a) Particles/cells will migrate to acoustic energy maxima/minima depending on their acoustic contrast with the media in which they are suspended. (b) The acoustic contrast factor can be modified for a given particle type by altering the acoustic properties of the surrounding media. Red blood cells (RBCs) can have an acoustic contrast factor that is positive or negative depending on the optiprep concentration, where optiprep contains 60% w/v iodixanol. The range of literature RBC density and compressibility values range from $\rho = 1.078$ g/cm³, $\beta = 3.91e-10$ Pa⁻¹ (lower density RBCs) to $\rho = 1.096$ g/cm³, $\beta = 3.48e-10$ Pa⁻¹ 1,2,3,4. All optiprep concentrations above $\approx 56\%$ result in negative acoustic contrast factors for this indicated range.

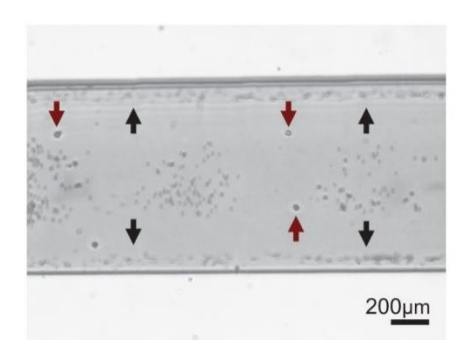


Figure S2: (a) RBCs (0.5% v/v) and 1.1 μm PS particles in 95% Optiprep media. RBCs show negative acoustic contrast (red arrow) and particles have positive acoustic contrast (black arrow) under zero-flow conditions.

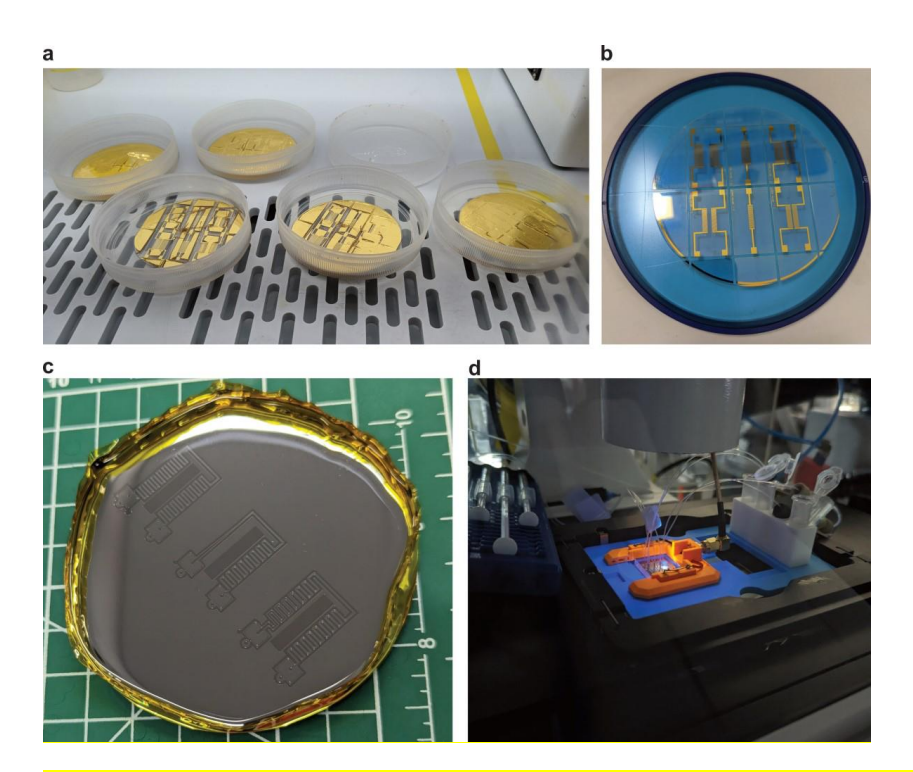


Figure S3: Acoustic sorting device fabrication. a) Wet etching in acetone to lift off Cr-Au-Cr material deposited on photoresist patterned areas. b) Wafer diced into individual transducers. c) Moulding PDMS on SU8 patterned silicon wafer wrapped in Kapton tape. d) Device assembled on the microscope placed in 3D printed holder with magnetically attached electrode connections.

References

- 1. Dai, H. & Feng, R. Ultrasonic attenuation in red blood cell suspensions. *Ultrasonics* **26**, 168–170 (1988).
- 2. Kuo, I. Y. & Shung, K. K. High frequency ultrasonic backscatter from erythrocyte suspension. *IEEE Trans Biomed Eng* **41**, 29–34 (2002).
- 3. Dukhin, A. S., Goetz, P. J. & van de Ven, T. G. M. Ultrasonic characterization of proteins and blood cells. *Colloids Surf B Biointerfaces* **53**, 121–126 (2006).
- 4. D'Alessandro, A., Blasi, B., D'Amici, G. M., Marrocco, C. & Zolla, L. Red blood cell subpopulations in freshly drawn blood: application of proteomics and metabolomics to a decades-long biological issue. *Blood transfusion* 11, 75 (2013).
- 5. Wilson, D. W., Crabb, B. S. & Beeson, J. G. Development of fluorescent Plasmodium falciparum for in vitro growth inhibition assays. *Malar J* **9**, 1–12 (2010).